The following publication J. M. Rocamora, I. W. -H. Ho and M. -W. Mak, "The Application of Machine Learning Techniques on Channel Frequency Response Based Indoor Positioning in Dynamic Environments," 2018 IEEE International Conference on Sensing, Communication and Networking (SECON Workshops), Hong Kong, China, 2018 is available at https://doi.org/10.1109/SECONW.2018.8396358.

The Application of Machine Learning Techniques on Channel Frequency Response based Indoor Positioning in Dynamic Environments

Josyl Mariela Rocamora*†, Ivan Wang-Hei Ho*‡ and Man-Wai Mak*
*Department of Electronic and Information Engineering, The Hong Kong Polytechnic University
‡The Hong Kong Polytechnic University Shenzhen Research Institute
†Department of Electronics Engineering, University of Santo Tomas, Philippines
josyl.rocamora@connect.polyu.hk, {ivanwh.ho, enmwmak}@polyu.edu.hk

***Abstract*—Traditional IPS uses triangulation based on signal strength but its accuracy is impaired in non-line-of-sight (NLOS) situations. Among the available wireless technologies for indoor positioning, WiFi is a good candidate since it is supported by existing mobile devices and indoor infrastructure, and it can operate under both LOS and NLOS conditions. One of the cutting-edge WiFi-based localization techniques exploits time-reversal resonating strength (TRRS) of coherent channel frequency responses (CFR). CFR-based positioning is based on the similarity measure between the testing CFR and the pre-recorded CFR fingerprints. A common assumption in previous works is that wireless channels are time invariant. In this paper, we study CFR-based positioning in a dynamic indoor environment. Using the collected channel response fingerprints for both LOS and NLOS scenarios, we exploit supervised machine learning techniques to speed up the positioning process while achieving high positioning accuracy under the effect of dynamic wireless channels.**

***Index Terms*—Indoor Positioning System (IPS), Channel Frequency Response (CFR), Support Vector Machine (SVM)**

I. Introduction to Indoor Positioning System

The Internet-of-Things (IoT) comprises numerous networked electronic devices, tags and sensors. With a massive number of IoT-connected devices, it would be impractical to broadcast a message to all of them. Therefore, locating the device for receiving an information is important in this vast network. This will enable applications such as monitoring, navigation and location-based network access [1], [2].

Localizing mobile devices in an outdoor environment typically utilizes the Global Positioning System (GPS). On the other hand, there are several methods of localizing devices in an indoor environment and these can be classified either as active or passive indoor positioning systems (IPS) [1].

Active IPS involves wireless technologies such as Radio Frequency Identification (RFID), Bluetooth, Ultra-wideband (UWB), IEEE 802.11 (WiFi), etc., as discussed in a survey [1]. Among the available active IPS, WiFi is a good choice for indoor localization as it offers medium to high accuracy even under NLOS situations and can be readily supported by existing mobile devices and indoor infrastructure.

This work is supported in part by the National Natural Science Foundation of China (Project No. 61401384); and by The Hong Kong Polytechnic University (Projects 4-ZZCZ, G-YBXJ).

Localization using WiFi involves mapping wireless measurements into a more comparable set of parameters [3]. Received Signal Strength Indicator (RSSI) is one of the typical measurements [4]. Traditional localization techniques use geographic mapping of relative distances and directions from fixed WiFi access points and convert these features into locations using algorithms such as triangulation [2], [3]. This approach is straightforward but is dependent on the availability of LOS since the signal strength is highly affected by obstructions. Therefore, the localization accuracy suffers when the environment is rich in multi-path effects and fading.

Recent efforts on localization in an NLOS environment employ a technique called Time Reversal Resonating Strength (TRRS) based on the Channel State Information (CSI) of a wireless channel [5]–[8]. Unlike RSSI, CSI is a physical (PHY) layer feature that can characterize the multi-path effects of NLOS conditions. It has two types namely, Channel Impulse Response (CIR) for time-domain representation of the complex channel and Channel Frequency Response (CFR) for the frequency-domain counterpart. Since TRRS assumes a linear time-invariant channel (LTI), research in this area focuses on a relatively static environment.

In this research, we aim to investigate CFR-based IPS in a dynamic environment. The main contributions are as follows:

- We investigate the performance of CFR-based positioning in both LOS and NLOS conditions.
- We analyze the behavior of a temporally dynamic environment using CFR fingerprints.
- We demonstrate that applying a supervised learning technique can boost the processing speed while maintaining high-accuracy localization of CFR-based positioning.

II. CFR-based IPS using TRRS

TRRS is regarded as a measure of similarity between two CSI fingerprints [5]–[8]. Based on the time reversal signal processing principle, the channel is assumed to be linear time invariant, that is, the channel is reciprocal and static. When comparing two fingerprints from the same wireless channel (i.e. same location) with TRRS, the temporal-spatial focusing effect will be triggered and results in a highly focused impulse.

TRRS in frequency domain $\gamma[\hat{\mathbf{H}}, \hat{\mathbf{H}}']$ of two CFR fingerprints is expressed in (1) and its computation is less complex compared to that in the time domain [7]. For instance, the convolution in time domain is simply a multiplication in frequency domain.

$$\gamma[\hat{\mathbf{H}}, \hat{\mathbf{H}}'] = \frac{|\sum_{k=1}^{K} \hat{H}_{u_k} \hat{H}'_{u_k}|^2}{\langle \hat{\mathbf{H}}, \hat{\mathbf{H}} \rangle \langle \hat{\mathbf{H}}', \hat{\mathbf{H}}' \rangle} \tag{1}$$

We can view $\hat{\mathbf{H}}$ as the CFR fingerprint of a known location (training data) previously recorded in the database while $\hat{\mathbf{H}}'$ as an extracted CFR fingerprint of an unknown location (testing data). The testing fingerprint will be matched to historical fingerprints in the database. The location of the training fingerprint that yields the highest numerical value of TRRS would be regarded as the position of the testing fingerprint.

Table I lists recent works on TRRS and CSI fingerprints in NLOS environments with centimeter-level accuracy. Aside from TRRS, some previous works employed additional techniques like phase compensation (PC) as CFRs accumulate phase rotations over time, frequency-hopping method (FH) for collecting CFRs from multiple channels, and multiple transmit/receive antennas to generate and combine CFRs. When evaluating the localization performance of these previous works, the considered environment is relatively static, that is the coherence time of the channel is long enough as not to cause large temporal variations.

TABLE I
EXISTING WORKS ON TRRS/CSIS IN NLOS CONDITIONS

Ref.	CSI	Accuracy	Bandwidth	Techniques
[5]	CIR	10 cm	125 MHz	TRRS
[6]	CFR	5 cm	1 GHz	TRRS, PC
[7]	CFR	5 cm	1 GHz	TRRS, PC, FH
[8]	CFR	5 cm	1 GHz	TRRS, PC, FH, Multi-TX/RX

Table II summarizes the channel stationarity tests of previous related works.[1] Based on the table, the TRRS decays with time. CFR fingerprints may have a TRRS as low as 0.56 (the maximum value is 1) if separated by three days [8]. When there are nearby human activities, TRRS also suffers. If the person opens and closes the door, TRRS of the target location can go as low as 0.50 while the TRRS of other locations can go as high as 0.50 [8].

TABLE II
CHANNEL STATIONARITY (SELF-TESTS)

Ref.	CSI	Test	Approx TRRS
[5]	CIR	Time (18 hours)	> 0.80
[5]	CIR	Human presence (few min)	> 0.80
[9]	CIR	Time (20 min)	> 0.95
[9]	CIR	Human presence (few min)	> 0.75
[8]	CFR	Time (97 hours)	> 0.56
[8]	CFR	Human presence (8-10 ft away)	> 0.53
[8]	CFR	Door movement	> 0.50

[1]TRRS values indicated in the table for [5] are only approximated values since their results only show colored charts and scales.

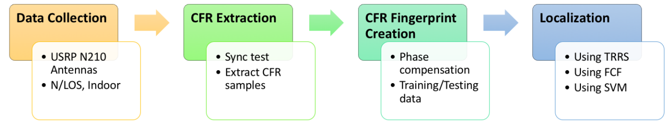

Fig. 1. Overview of the Research Methodology

In our previous work [10], the effects of the temporal variations were remedied by fingerprint appending and averaging. However, the study focused solely on the time component. In this work, we show that the TRRS does not only decay with time but is also affected by the environmental changes like the inclusion of obstructions or scatterers. We then employ a supervised machine learning algorithm to tackle such problem.

III. METHODOLOGY

Fig. 1 shows the block diagram of the research methodology.

A. Experimental Setup and Data Collection

Fig. 2 displays the setup inside a conference room of the data collection on March 18, 2018. The setup used USRP N210 devices similar to our previous work [10]. Two devices were used: the access point (AP) as the receiver while the target indoor localization (IL) as the transmitter. The USRPs were around 5 m apart and obstructed by a stack of chairs for the NLOS condition. We collected the CFRs of 4 different locations of the IL, which are the corners of a 30 cm by 30 cm square on top of a table similar to our previous work [10]. We collected data for four 2-hour periods. The first three periods were for NLOS conditions. The last period was for LOS condition, where the stacks of chairs between the antennas were removed. Table III lists the GRC parameter values used.[2]

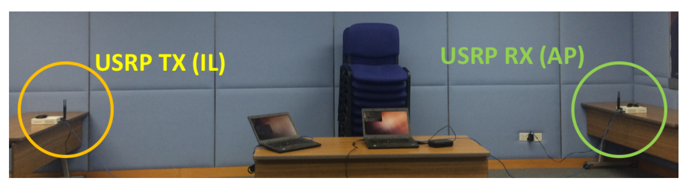

Fig. 2. NLOS scenario setup with 2 USRP N210 antenna modules

TABLE III
GNU RADIO COMPANION (GRC) SOFTWARE PARAMETERS

Parameter	Value
Sampling rate	12.5 MHz
Ch0 Antenna Gain, Type	25 dB, TX/RX
Ch0 Center Freq	3.42:0.01:3.78 GHz (10 MHz/channel)
(variable)	except 3.49-3.51, 3.59-3.61, 3.69-3.71
	Changed using FH method in [7]

B. CFR Extraction and Fingerprinting

CFR post-processing is based on the methods of [7] as shown in Fig. 3. We configured the sifting parameter $\tau = 0$.

For each 2-hour collection period, we generated 400 fingerprints (100 fingerprints per location). In total, we have 1600 fingerprints. A fingerprint is represented as $fp(i,L)$, where i is

[2]Some channels are excluded due to the presence of noticeable interference.

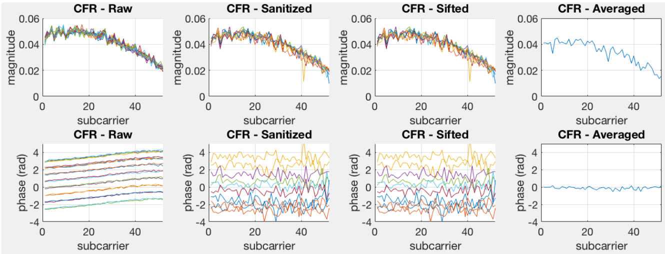

Fig. 3. Post processing applied to CFRs of channel 28, location 1 which are collected during NLOS - Period 1

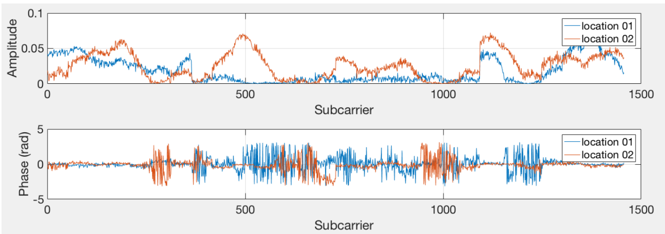

Fig. 4. Fingerprints from two locations collected during NLOS Period 1

the fingerprint number and L is the target location. Fingerprints $fp(1{:}100,L)$ are based on NLOS period 1, $fp(101{:}200,L)$ are based on NLOS period 2, $fp(201{:}300,L)$ are based on NLOS period 3, and $fp(301{:}400,L)$ are based on LOS period 4. In each period, two succeeding fingerprints are 4 ms apart, hence, all 100 fingerprints per location represent a 4 sec time separation.

Fig. 4 shows the complex CFR fingerprints taken from two different locations, $fp(1,1)$ and $fp(1,2)$. Both locations have unique CFR fingerprints. The erratic phase is attributed to very low magnitude for some of the bands within the spectrum.

C. Localization Techniques

For single training and single testing scenarios, TRRS is calculated based on (1). Since introducing more training data can improve the positioning performance, we utilized two remedies namely, Continuous Fingerprint Appending (CFA) and Weighted Fingerprint Averaging (WFA) proposed in [10].

Apart from TRRS, we also introduced the use of machine learning techniques like Support Vector Machines (SVM) to identify the hidden properties within the fingerprints for positioning. Each location is treated as one class. The number of training (testing) data input to the SVM is the number of training (testing) fingerprints multiply the number of classes. In this paper, we utilize a multi-class SVM with the following kernel functions: Linear, Quadratic, Polynomial (degree 3), and Gaussian radial basis function (rbf) with $\sigma = 6$.

Before using the SVM, Principal Component Analysis (PCA) was applied to each normalized fingerprint. Since CFRs are complex-valued, we treated the real and imaginary parts as separate features. The optimal number of features or principal components (PC) used for a particular SVM was identified so as to maximize the overall accuracy.

For multiple training and testing, we performed leave-one-period-out cross validation to avoid selection bias. Since we

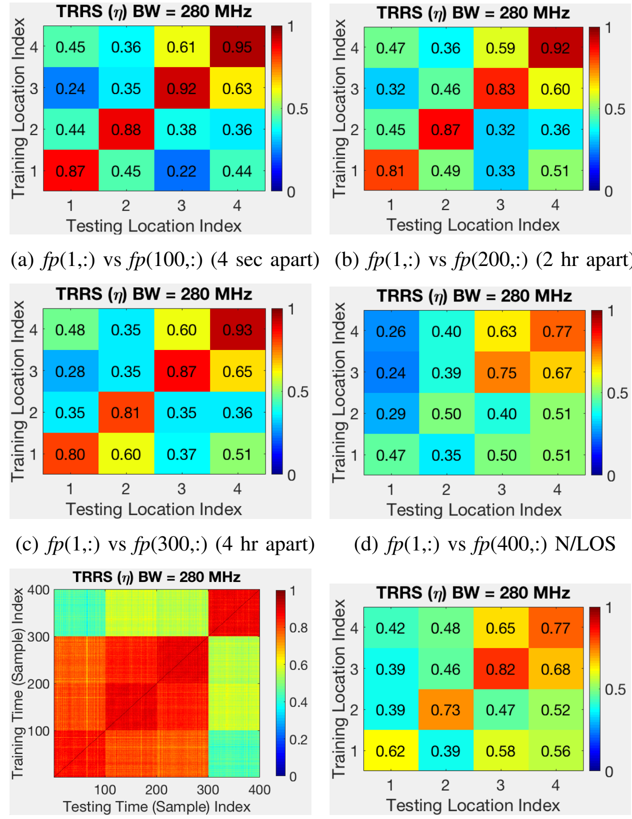

(a) $fp(1,:)$ vs $fp(100,:)$ (4 sec apart) (b) $fp(1,:)$ vs $fp(200,:)$ (2 hr apart)

(c) $fp(1,:)$ vs $fp(300,:)$ (4 hr apart) (d) $fp(1,:)$ vs $fp(400,:)$ N/LOS

(e) $fp(:,1)$ vs $fp(:,1)$ (varying time) (f) $fp(1{:}300,:)$ vs $fp(400,:)$ N/LOS

Fig. 5. TRRS Matrix: Training Data vs Testing Data

have four collection periods, we performed four cross validation experiments. Experiments 1 to 4 use 400 fingerprints $fp(1{:}100,:)$, $fp(101{:}200,:)$, $fp(201{:}300,:)$ and $fp(301{:}400,:)$, respectively, as testing data, while the remaining 1200 fingerprints as training data. Experiment 4 of the cross validation considers fingerprint matching of LOS testing fingerprints to NLOS training fingerprints.

IV. Data and Results

A. TRRS and Channel Dynamics

Fig. 5 displays various TRRS matrices. Figs. 5(a) to 5(c) show the TRRS for NLOS scenarios when $fp(1,:)$ is the training data while $fp(i,:)$ is the testing data. Fig. 5(d) shows the TRRS when an NLOS fingerprint is used for training while an LOS fingerprint is used for testing. The high TRRS values on the diagonals indicate that the algorithm is able to correctly localize each location. However, we can see that the diagonal TRRS values drop significantly in Fig. 5(d), because this case uses NLOS fingerprints as training data and LOS fingerprints as testing data.

Fig. 5(e) shows a self-test for $fp(:,1)$. This figure suggests that NLOS fingerprints $fp(1{:}300,1)$ are highly correlated with each other but are less correlated with the LOS fingerprints $fp(301{:}400,1)$. Fig. 6 depicts how the TRRS decays when we tested each fingerprint against $fp(1,:)$. The average value of the TRRS matrix diagonal elements decreases with time and as

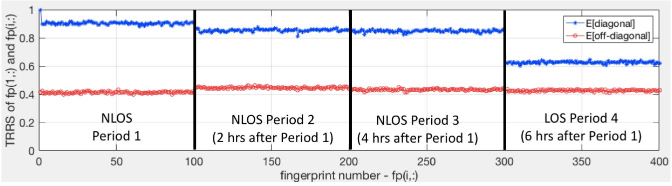

Fig. 6. Average values of the diagonal and off-diagonal elements in the TRRS of the 1st fingerprint vs the i-th fingerprint

the situation changes from NLOS to LOS as expected because TRRS assumes an LTI channel. To mitigate this problem, we employed the CFA remedy proposed in [10] and calculated the TRRS with all 1200 NLOS fingerprints *fp*(1:300,:) as training data and 4 LOS fingerprints *fp*(400,:) as testing data. As shown in Fig. 5(f), TRRS of the diagonal elements have considerably improved.

B. TRRS and SVM

For each localization technique, we calculated the location prediction accuracy using leave-one-period-out cross validations as shown in Table IV. We also consider the processing time for localization.

TABLE IV
PERFORMANCE OF VARIOUS LOCALIZATION TECHNIQUES BASED ON LEAVE-ONE-PERIOD-OUT CROSS VALIDATION

Period	Accuracy (0 to 1) for each period 1	2	3	4 (LOS)	Overall	Time (sec)
CFA	1.0000	1.0000	1.0000	1.0000	1.0000	38.9
WFA	0.6575	0.9925	0.9975	0.9975	0.9113	30.1
Linear	1.0000	1.0000	1.0000	1.0000	1.0000	12.0
Quad	1.0000	1.0000	1.0000	0.7625	0.9406	21.6
Poly(3)	1.0000	1.0000	1.0000	0.9950	0.9988	15.0
Rbf(6)	1.0000	1.0000	1.0000	0.9975	0.9994	23.8

TRRS with CFA has 100% localization but requires the longest time to process since the method matches a testing fingerprint to each of the fingerprints in the database. TRRS with WFA has poor accuracy since it uses the weighted average of the historical fingerprints, that is, giving more importance to more recent fingerprints.

In Experiment 1, Period 1 fingerprints are testing data. Period 4 fingerprints are most recent and are given more weight in WFA. Based on Fig. 5(d), fingerprints from Periods 1 and 4 have low correlation. WFA-averaged fingerprints are therefore less correlated to the testing fingerprints. This explains the low accuracy of 65.75%. The unique CFR characteristics is hence discounted by this averaging technique.

Looking at the SVM-based techniques, the linear SVM has perfect accuracy and fast computation which indicates that our data are linearly separable. Other types of SVM still exhibit good results with relatively fast processing time. Inaccurate localization is only exhibited during period 4, since we are testing LOS fingerprints against NLOS fingerprints.

In real-world applications, localization must be computationally efficient for several reasons. First, WiFi access point concurrently acts as the communication gateway and positioning server for multiple end devices that could be moving fast. Second, the training database for numerous target positions can be of considerable size. Therefore, it is most desirable that the positioning technique can instantaneously classify the fingerprint of an unknown target location.

V. CONCLUSION AND FUTURE WORK

We have shown that existing WiFi IPS based on TRRS can localize devices using CFR signatures. Since TRRS assumes an LTI channel, its performance may degrade over time and suffer when the environment has changed, that is, the change of the scatterers' positions.

For our collected CFR fingerprints in both indoor NLOS and LOS environments, the TRRS with CFA and SVM techniques have shown high accuracy in determining the position of 400 LOS testing fingerprints based on 1200 NLOS training fingerprints. TRRS techniques can be improved through fingerprint averaging and achieve good localization performance at the expense of long processing time. This motivated us to introduce the multi-class linear SVM technique that can provide perfect performance with significantly faster computation speed (around 30% of the time needed by TRRS with CFA).

Because of its low computational complexity and high accuracy, we aim to further investigate the use of multi-class linear SVM for IPS in a larger scale. For instance, we can expand our work to consider the tracking of moving objects in a dynamic environment. To achieve this, we must be able to perform localization across a greater number of positions.

REFERENCES

[1] G. Deak, K. Curran, and J. Condell, "A survey of active and passive indoor localisation systems," *Computer Communications*, vol. 35, no. 16, pp. 1939 – 1954, 2012.

[2] A. Makki, A. Siddig, M. Saad, and C. Bleakley, "Survey of wifi positioning using time-based techniques," *Computer Networks*, vol. 88, no. Supplement C, pp. 218 – 233, 2015.

[3] Z. Yang, Z. Zhou, and Y. Liu, "From rssi to csi: Indoor localization via channel response," *ACM Comput. Surv.*, vol. 46, no. 2, pp. 25:1–25:32, Dec. 2013.

[4] Z. Situ, I. W.-H. Ho, H. C. B. Chan, and D. P. K. Lun, "The impact of node reliability on indoor cooperative positioning," in *2016 IEEE International Conference on Digital Signal Processing (DSP)*, Oct 2016, pp. 300–304.

[5] Z. H. Wu, Y. Han, Y. Chen, and K. J. R. Liu, "A time-reversal paradigm for indoor positioning system," *IEEE Transactions on Vehicular Technology*, vol. 64, no. 4, pp. 1331–1339, April 2015.

[6] C. Chen, Y. Chen, H. Q. Lai, Y. Han, and K. J. R. Liu, "High accuracy indoor localization: A wifi-based approach," in *2016 IEEE International Conference on Acoustics, Speech and Signal Processing (ICASSP)*, March 2016, pp. 6245–6249.

[7] C. Chen, Y. Chen, Y. Han, H. Q. Lai, and K. J. R. Liu, "Achieving centimeter-accuracy indoor localization on wifi platforms: A frequency hopping approach," *IEEE Internet of Things Journal*, vol. 4, no. 1, pp. 111–121, Feb 2017.

[8] C. Chen, Y. Chen, Y. Han, H. Q. Lai, F. Zhang, and K. J. R. Liu, "Achieving centimeter-accuracy indoor localization on wifi platforms: A multi-antenna approach," *IEEE Internet of Things Journal*, vol. 4, no. 1, pp. 122–134, Feb 2017.

[9] B. Wang, Y. Wu, F. Han, Y. H. Yang, and K. J. R. Liu, "Green wireless communications: A time-reversal paradigm," *IEEE Journal on Selected Areas in Communications*, vol. 29, no. 8, pp. 1698–1710, Sep 2011.

[10] E. R. Magsino, I. W. H. Ho, and Z. Situ, "The effects of dynamic environment on channel frequency response-based indoor positioning," in *2017 IEEE 28th Annual International Symposium on Personal, Indoor, and Mobile Radio Communications (PIMRC)*, Oct 2017, pp. 1–6.